*Korean J. Chem. Eng.*, **31**(11), 1980-1984 (2014)
DOI: 10.1007/s11814-014-0144-x

pISSN: 0256-1115
eISSN: 1975-7220

# The effect of loading on sintering and catalytic activity of $Pt/SiO_2$ hybrid catalyst powders synthesized via spray pyrolysis

**Jaecheol Yun*,***,‡, Chan-Ho Jung***,****,‡, Dahee Park*, Hye Young Koo*, Jung-Yeul Yun*, Yangdo Kim**,†, and Jeong Young Park***,****,†**

*Powder Technology Department, Korea Institute of Materials Science (KIMS), Changwon 642-831, Korea
**Department of Material Science and Engineering, Pusan National University, Busan 607-735, Korea
***Center for Nanomaterials and Chemical Reactions, Institute for Basic Science (IBS), Daejeon 305-701, Korea
****Graduate School of EEWS, Korea Advanced Institute of Science and Technology (KAIST), Daejeon 305-701, Korea
(*Received 21 March 2014 • accepted 21 May 2014*)

**Abstract**−Platinum (Pt) is commonly used as a heterogeneous catalyst to effectively convert carbon monoxide (CO) from automobile exhaust gas into carbon dioxide ($CO_2$). Platinum/silica ($Pt/SiO_2$) hybrid catalyst powders with varying Pt content were synthesized via a spray pyrolysis process. The average particle size and specific surface area of the Pt nanoparticles on the $Pt/SiO_2$ hybrid catalyst powders were characterized as-prepared and after heat treatment. As the Pt loading increased, the Pt nanoparticles grew on the surface of the $SiO_2$ as a result of sintering, and the catalytic efficiency decreased. This work demonstrates that the $Pt/SiO_2$ (4 wt% Pt) hybrid catalyst powder is suitable as a high-temperature automobile exhaust catalyst, compared with the $Pt/SiO_2$ hybrid catalyst powder with high Pt loading (14 wt% Pt), indicating that metal nanoparticle loading is a key factor for determining catalytic activity.

Keywords: Spray Pyrolysis Process, Hybrid Catalyst Powder, Pt Nanoparticles, CO Oxidation

## INTRODUCTION

Metal-supported oxide hybrid catalysts are promising heterogeneous catalysts because of possible synergistic effects on catalytic activity due to metal-support interactions [1-4]. These catalysts are used for practical applications, including purification of hydrogen for proton exchange membrane fuel cells and reduction of toxic carbon monoxide (CO) gas from automobile exhaust gases [5-11]. Noble metals have been studied for applications as heterogeneous hybrid catalysts due to their excellent catalytic activities and stabilities [11]. In particular, Pt nanoparticle-supported oxide catalysts have been widely used for CO oxidation reactions for the past few years [12-20]. Catalyst synthesis methods usually involve wet chemical processes (e.g., sol-gel, deposition precipitation, co-precipitation) where the organic agent or surfactant may be used to control the size, shape, and composition of the catalytic nanoparticles [21-24]. However, catalysts fabricated using wet chemical methods have low thermal stability above 300 °C and it is difficult to maintain the original structure because the organic agent or surfactant decomposes. Therefore, catalysts fabricated by a wet chemical method exhibit limited performance under high-temperature reactions, such as CO oxidation [25], hydrocarbon cracking [26], combustion [27], partial oxidation [28], and ignition behavior studies [29]. Wet chemical methods also require a long time to prepare the catalysts and can only produce a small quantity of catalysts at a time. Hence, for large-scale fabrication, physical methods are used more often than chemical methods. Physical methods (e.g., spray pyrolysis [30,31], electrical wire explosion [32], vapor deposition [33], laser ablation [34]) can easily fabricate catalysts. Considering the demand for rapid, easy, and large-scale catalyst fabrication, the spray pyrolysis process is a promising method for producing new conceptual hybrid catalysts.

Spray pyrolysis is a general process for synthesizing desired nanomaterials by decomposing a precursor solution at high temperature. Spray pyrolysis has inherent advantages over other processes. Homogeneous mixing of the precursor and short residence times in the reactor can produce uniform-phase, high-purity, and multicomponent powders [31]. The spray pyrolysis process consists of a storage tank for the precursor, a nebulizer to make droplets, a reactor, and a bag filter unit. During synthesis, precursor droplets atomized by a nebulizer continuously transfer in the high-temperature reactor using the carrier gas. The droplets then form the desired particles through evaporation, thermal decomposition, and crystallization [30,31,35]. By controlling process variables (e.g., reaction temperature, flow rate, and concentration of the precursor solutions), various kinds of hybrid catalysts can be designed using spray pyrolysis. Industry prefers the spray pyrolysis process for its simplicity, low cost, variety, and reproducibility [35]. In this study, we synthesized $Pt/SiO_2$ hybrid catalyst powders with two Pt contents (4 and 14 wt% Pt) using the spray pyrolysis process, and studied the effect of Pt loading on sintering and catalytic activity. To control the loading amount, we changed the concentration of the Pt precursor solution. We used heat treatment for 30 minutes at 600 °C in air to improve the thermal stability of the fabricated $Pt/SiO_2$ hybrid catalyst powders. The catalytic activities of the $Pt/SiO_2$ hybrid catalyst powders were evaluated at 100% CO conversion, where we looked for the optimal Pt content.

†To whom correspondence should be addressed.
E-mail: jeongypark@kaist.ac.kr, yangdo@pusan.ac.kr
‡Equally contributed

## EXPERIMENTAL

### 1. Preparation of $Pt/SiO_2$ Catalyst Powders

The $Pt/SiO_2$ hybrid catalyst powders were synthesized via spray pyrolysis. Chloroplatinic acid hexahydrate ($H_2Cl_6Pt{\cdot}6H_2O$, Aldrich) and fumed silica ($SiO_2$, Aldrich) were used as the Pt precursor and support, respectively. The $SiO_2$ particles were about 0.2-0.3 μm in size. The spray solution was prepared thus: Two solutions were prepared where 2.0 g $SiO_2$ was diluted in 100 mL water, and the intended amounts of $H_2Cl_6Pt{\cdot}6H_2O$ were also dissolved in 100 mL water (5 wt% and 20 wt%). The spray solution was prepared by mixing the two solutions with a stirrer at room temperature and then immediately sonicated for 10 minutes. In the spray pyrolysis process, droplets formed through the nebulizer were transferred to a quartz tube reactor (1,000 mm length and 100 mm internal diameter) at 500 °C and a flow rate of 50 L/min using compressed air. The $Pt/SiO_2$ hybrid catalyst powders were synthesized and then collected from the bag filter. We heat-treated the $Pt/SiO_2$ hybrid catalyst powders at 600 °C for 30 minutes in air to enhance fixation of the Pt nanoparticles on the surface of the $SiO_2$ powder. A flow diagram for the $Pt/SiO_2$ hybrid catalyst powder synthesis is shown in Fig. 1.

### 2. Characterization of $Pt/SiO_2$ Powders

The morphology and size of the Pt nanoparticles dispersed on the surface of the $SiO_2$ powder were observed using a transmission electron microscope (TEM, JEOL, JEM-2100F, 200 kV). An X-ray diffractometer (XRD, Rigaku, D/Max 2200) was used to confirm the crystallinity of the Pt nanoparticles on the $SiO_2$ powder. The amount of Pt in the $Pt/SiO_2$ hybrid catalyst powder was measured via inductively coupled plasma optical emission spectrometry (ICP-OES, PerkinElmer, Optima 8300). The flow reactor system was used to measure the critical temperature of 100% CO conversion. About 100 mg of catalyst was loaded into a quartz tube. The hybrid catalyst powder was reduced at 250 °C under $H_2$ flow (5% $H_2$ in He at 45 mL/min) for 30 min and then cooled to room temperature. The reactant gas composition was 4% CO, 10% $O_2$, and 86% He (balance). The total gas flow rate was 50 mL/min, controlled by mass flow controllers (BROOKS instrument). CO oxidation was carried out until 100% CO conversion was reached in the temperature range of 80-260 °C. There was no CO conversion observed in the empty reactor. The gas mixture passing through the catalyst powder was analyzed using gas chromatography (GC; DS science).

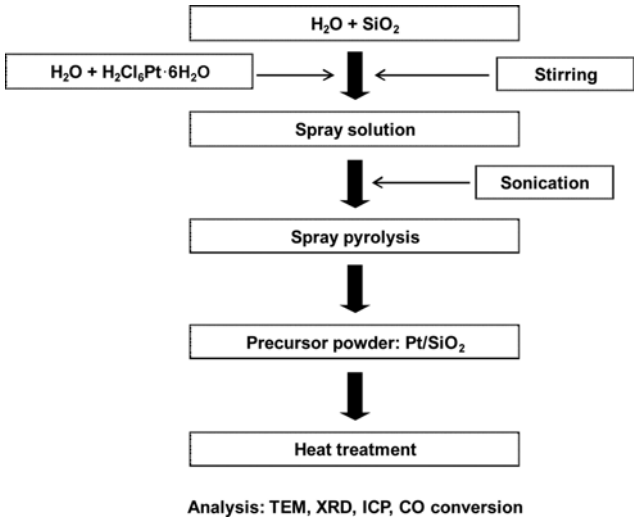


**Fig. 1. Flow diagram for the synthesis of $Pt/SiO_2$ hybrid catalyst powders using the spray pyrolysis process.**

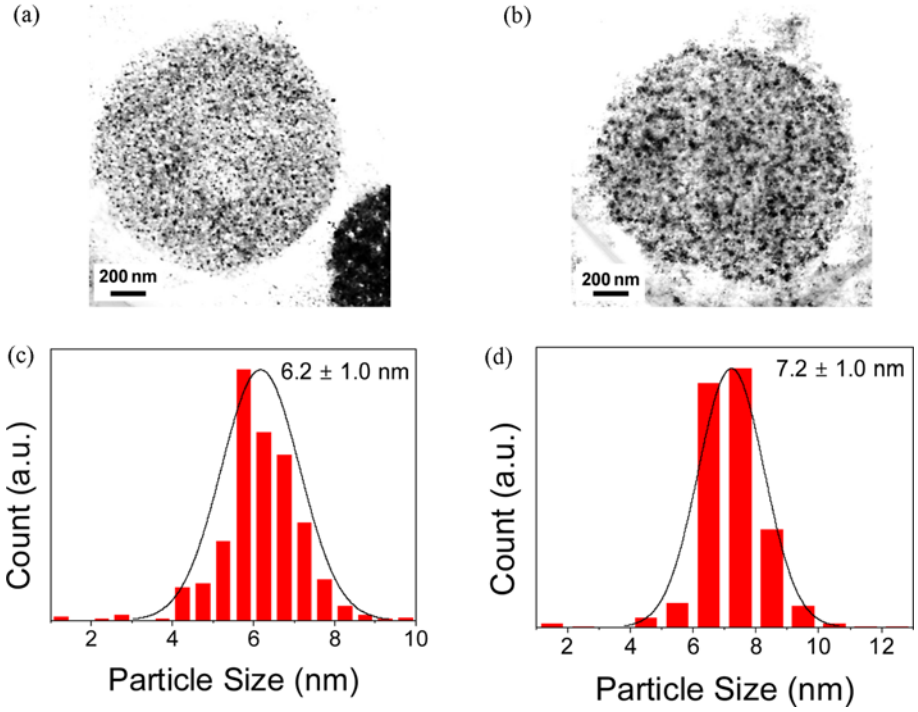


**Fig. 2. (a), (b) TEM images and (c), (d) size distributions of 4 and 14 wt% $Pt/SiO_2$ hybrid catalyst powders synthesized via spray pyrolysis, respectively.**

**Table 1. Results of chemisorption measurement on $Pt/SiO_2$ hybrid catalyst powders**

| | 4 wt% As-prepared | 14 wt% As-prepared | 4 wt% Heat-treated | 14 wt% Heat-treated |
|---|---|---|---|---|
| Metal surface area per sample weight ($m^2/g$) | 2.6218 | 3.7383 | 0.6507 | 0.0145 |

## RESULTS AND DISCUSSION

### 1. Catalyst Characterization

Fig. 2 shows TEM images and size distributions of the Pt nanoparticles on the $Pt/SiO_2$ hybrid catalyst powders fabricated via spray pyrolysis. As the Pt content increased from 4 to 14 wt%, the Pt nanoparticles increased in size from 6.2 to 7.2 nm, the metal surface area per sample weight increased from 2.62 to 3.74 $m^2/g$ (Table 1). The droplets generated by the nebulizer in the spray pyrolysis process, which involves the Pt precursor and $SiO_2$ powder, were passed through a furnace. The Pt nanoparticles dispersed on the surface of the $SiO_2$ were synthesized by Pt precursor decomposition, solvent evaporation, and the nucleation and growth of the Pt nanoparticles. We assumed that the average size, area density, and surface area of the Pt nanoparticles increased with increasing Pt content because of the increased amount of Pt precursor contained in a single droplet generated by the nebulizer.

Fig. 3 shows TEM images and size distributions of the Pt nanoparticles on the heat-treated $Pt/SiO_2$ hybrid catalyst powders. As the Pt content increased from 4 to 14 wt%, the average size of the Pt nanoparticles increased from 13 to 27 nm and the Pt surface area per sample weight decreased from 0.6507 $m^2/g$ to 0.0145 $m^2/g$. The Pt surface area per sample weight decreased, compared with the as-prepared $Pt/SiO_2$ hybrid catalyst powders, due to sintering effects (nanoparticle collision, grain growth, agglomeration, fusion between large interconnected nanoparticles, etc.) [36-38]. The average size of the Pt nanoparticles synthesized from 14 wt% Pt became bigger after heat treatment than those synthesized from 4 wt% Pt due to sintering effects and higher particle densities.

Fig. 4 shows the XRD patterns for each $Pt/SiO_2$ hybrid catalyst powder prepared from 4 and 14 wt% Pt after heat treatment. The X-ray diffraction patterns of the $Pt/SiO_2$ hybrid catalyst powders have peaks observed with $2\theta$ values of 40.2°, 46.8°, 68.4°, 82.4°, and 87.0°; the crystallinity of the Pt was confirmed by the lattice structures of [111], [200], [220], [311], and [222]. As indicated above, the presence of pure crystalline Pt was confirmed after heat treatment regardless of the amount of Pt; meanwhile, the intensity of the Pt peaks increased and became sharper as the amount of Pt increased.

### 2. Catalytic Activity of Hybrid Catalysts

Fig. 5 compares the CO conversion rates of the $Pt/SiO_2$ hybrid catalyst powders with different Pt content before and after heat treatment. The critical temperatures of 100% CO conversion ($T_{100}$) for the $Pt/SiO_2$ hybrid catalyst powders synthesized with 4 and 14 wt% Pt were 180 and 150 °C, respectively. However, the $T_{100}$ of the heat-treated $Pt/SiO_2$ hybrid catalyst powders with 4 and 14 wt% Pt were 190 and 250 °C, respectively.

As shown in Table 1, the as-prepared $Pt/SiO_2$ hybrid catalyst powders have a higher Pt nanoparticle surface area than the heat-treated $Pt/SiO_2$ hybrid catalyst powders. After heat treatment, however, the specific surface area of the Pt nanoparticles decreased due to the sintering effect on the Pt nanoparticles dispersed on the $SiO_2$ surface. Therefore, the $T_{100}$ of the heat-treated $Pt/SiO_2$ hybrid catalyst

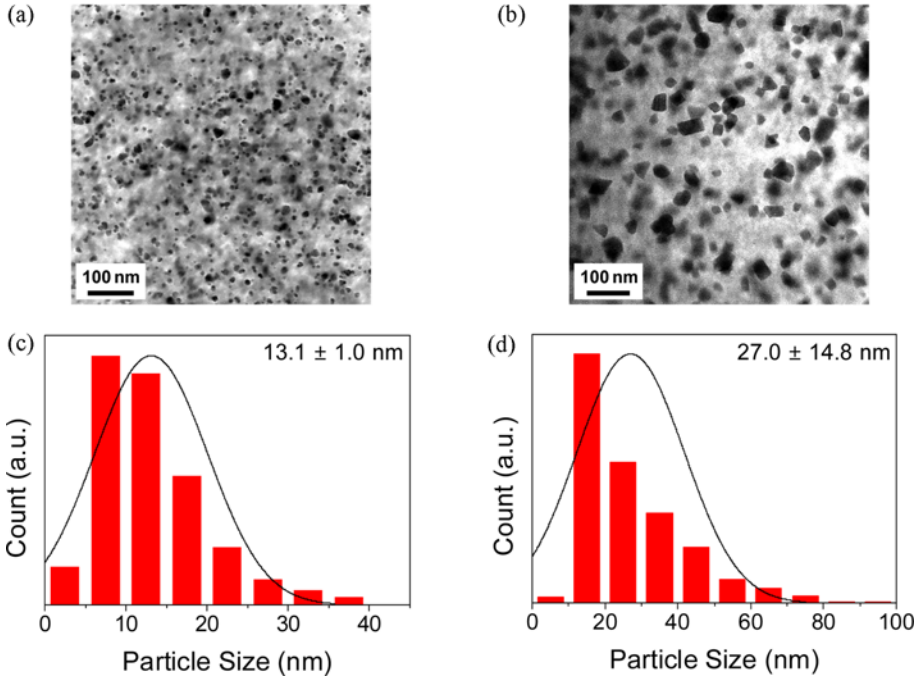


**Fig. 3. (a), (b) TEM images and (c), (d) size distributions of 4 and 14 wt% $Pt/SiO_2$ hybrid catalyst powders heat-treated at 600 °C in air, respectively.**

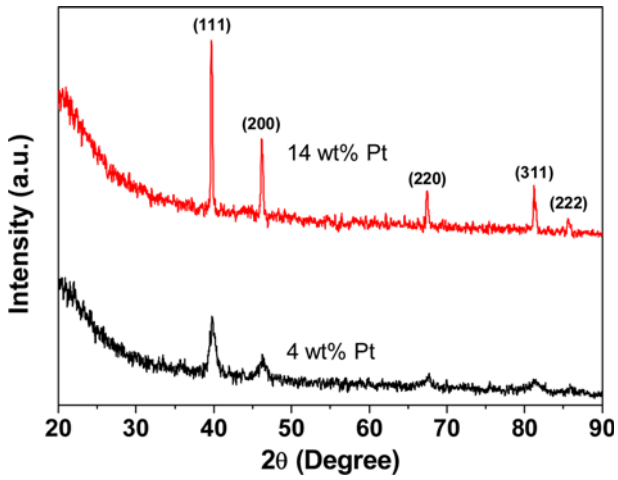


**Fig. 4. XRD patterns of 4 and 14 wt% Pt/$SiO_2$ hybrid catalyst powders heat-treated at 600 °C in air.**

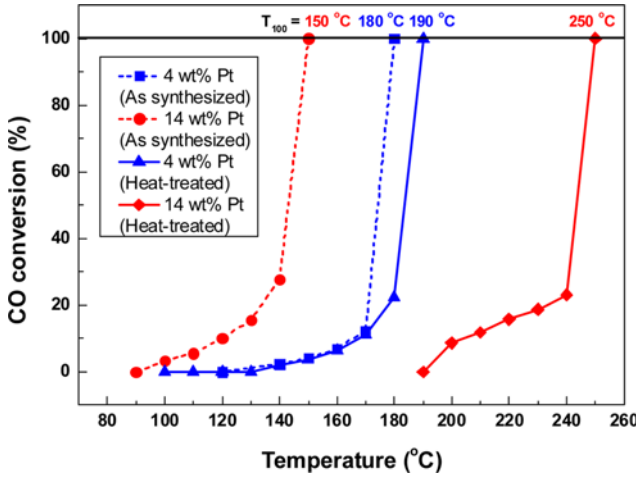


**Fig. 5. CO conversion results for the Pt/$SiO_2$ hybrid catalyst powders as-prepared and after heat treatment.**

powders was higher than the as-prepared Pt/$SiO_2$ hybrid catalyst powders. Fig. 5 shows that the Pt/$SiO_2$ hybrid catalyst powders synthesized with 14 wt% Pt lose catalytic activity after heat treatment because of the severe sintering that occurred on the catalysts. At high loading, agglomeration of the Pt nanoparticles during heating led to the creation of larger particles, resulting in a loss of Pt surface area and catalytic activity. On the other hand, the loss of catalytic activity of the Pt/$SiO_2$ hybrid catalyst powders synthesized with 4 wt% Pt is minimal. Consequently, the Pt/$SiO_2$ hybrid catalyst powders synthesized with 4 wt% Pt are more appropriate to use in automobile catalytic convertors at high temperature due to their excellent thermal stability. The fumed silica used as the support was stable after thermal treatment at high temperature. The TEM images do not show any degradation of the silica during high-temperature treatment. The drop in metal surface area for the 14 wt% Pt catalyst is mainly associated with sintering of the Pt nanoparticles, as confirmed by the TEM images and size distributions of the Pt nanoparticles (Fig. 2 and Fig. 3).

The catalytic activity of the Pt/$SiO_2$ nanocatalysts synthesized via spray pyrolysis exhibited high catalytic activity. For example, at 180 °C, we obtained a turnover frequency of 0.3 $s^{-1}$ for the 4 wt% Pt catalyst sample calcined at 600 °C for 30 min, which is higher than for a Pt/$SiO_2$ catalyst synthesized via wet chemical synthesis (0.1 $s^{-1}$ at 200 °C) [39]. We attribute this to better dispersion of the nanoparticles on the $SiO_2$ as well as good thermal stability of the nanocatalyst. This study suggests that metal loading plays an important role in controlling the sintering effect, and thus determining catalytic activity, indicating that optimized loading is a key factor for the smart design of catalytic materials.

Spray pyrolysis is known as a continuous process to synthesize metal or ceramic powders. Many metal materials (silver (Ag), copper (Cu), Nickel (Ni), copper/nickel and copper silver alloys) have been synthesized in a continuous-flow process using spray pyrolysis [40]. At laboratory scale, an ultrasonic nebulizer is usually used with frequencies on the order of 2 MHz. To increase production and spray of larger amounts from precursor solutions, industrial-scale setups are commercially available that can generate small droplets from precursor solutions using a high-intensity ultrasonic nebulizer. Also, the yield and the quality of the products can be maximized by adjusting several parameters including the flow rate of the carrier gas through the reactor, temperature inside the reactor, ultrasonic powder, solvents and chemical composition of the precursors. Due to these advantages, the spray pyrolysis process has potential applications in the commercial production of large amounts of catalyst material.

## CONCLUSION

Pt/$SiO_2$ hybrid catalyst powders with different Pt contents were synthesized via spray pyrolysis. The morphology, Pt nanoparticle size distribution, and crystallinity were measured using TEM and XRD, respectively. The Pt nanoparticles produced via spray pyrolysis were well dispersed on the $SiO_2$ powder. As the amount of Pt loaded on the $SiO_2$ powder increased, the average size, particle area density, and specific surface area of the Pt nanoparticles also increased. For CO conversion, the as-prepared Pt/$SiO_2$ hybrid catalyst powder with higher Pt content showed a lower $T_{100}$; however, after heat treatment, the $T_{100}$ showed the reverse phenomenon, indicating a loss of catalytic activity. Considering the use of a Pt/$SiO_2$ hybrid catalyst powder as a high-temperature automobile exhaust gas catalyst, the Pt/$SiO_2$ hybrid catalyst powder with 4 wt% Pt was more suitable than that with 14 wt% Pt, suggesting that metal loading optimization is a key factor for maximized catalytic activity.

## ACKNOWLEDGEMENTS

This work was supported by a grant from the Fundamental R&D Program for Core Technology of Materials funded by the Ministry of Trade, Industry & Energy, and by the Institute for Basic Science (IBS) [IBS-R004-G4-2014-a00], Republic of Korea.

## REFERENCES

1. G. A. Somorjai and J. Y. Park, *Angew. Chem. Int. Ed.*, **47**, 9212 (2008).
2. M. Haruta, N. Yamada, T. Kobayashi and S. Iijima, *J. Catal.*, **115**,

301 (1989).
3. S. J. Tauster and S. C. Fung, *J. Catal.*, **55**, 29 (1978).
4. D. W. Goodman, *Catal. Lett.*, **99**, 1 (2005).
5. S. Kim, K. Qadir, S. Jin, A. S. Reddy, B. Seo, B. S. Mun, S. H. Joo and J. Y. Park, *Catal. Today*, **185**, 131 (2012).
6. M. S. Chen, Y. Cai, Z. Yan, K. K. Gath, S. Axnanda and D. Wayne Goodman, *Surf. Sci.*, **601**, 5326 (2007).
7. B. Hvolbæk, Ton V. W. Janssens, Bjerne S. Clausen, H. Falsig, Claus H. Christensen and Jens K. Nørskov, *Nanotoday*, **2**, 4 (2007).
8. R. P. Eischens and W. A. Pliskin, *Adv. Catal.*, **9**, 662 (1957).
9. T. Engel and G. Ertl, *Adv. Catal.*, **28**, 1 (1979).
10. J. A. Rodriguez and D. W. Goodman, *Surf. Sci. Rep.*, **14**, 1 (1991).
11. N. W. Cant and D. E. Angove, *J. Catal.*, **97**, 36 (1986).
12. J. T. Kummer, *J. Phys. Chem.*, **90**, 4747 (1986).
13. A. S. Reddy, S. Kim, H. Y. Jeong, S. Jin, K. Qadir, K. Jung, C. H. Jung, J. Y. Yun, J. Y. Cheon, J.-M. Yang, S. H. Joo, O. Terasaki and J. Y. Park, *Chem. Commun.*, **47**, 8412 (2011).
14. S. H. Kim, C.-H. Jung, N. Sahu, D. Park, J. Y. Yun, H. Ha and J. Y. Park, *Appl. Catal. A: Gen.*, **454**, 53 (2013).
15. J. Y. Park, C. Aliaga, J. R. Renzas, H. Lee and G. Somorjai, *Catal. Lett.*, **129**, 1 (2009).
16. J. Y. Park, Y. Zhang, M. Grass, T. Zhang and G. A. Somorjai, *Nano Lett.*, **8**, 673 (2008).
17. M. Graham, M. Bär, I. Kevrekidis, K. Asakura, J. Lauterbach, H.-H. Rotermund and G. Ertl, *Phys. Rev. E*, **52**, 76 (1995).
18. J. Oi-Uchisawa, A. Obuchi, R. Enomoto, A. Ogata and S. Kushiyama, *Chem. Commun.*, 2255 (1998).
19. K. Qadir, S. H. Kim, S. M. Kim, H. Ha and J. Y. Park, *J. Phys. Chem. C*, **116**, 24054 (2012).
20. M. D. Graham, M. Bär and I. G. Kevrekidis, *Phys. Rev. E*, **52**, 1 (1995).
21. G. A. Somorjai, F. Tao and J. Y. Park, *Top. Catal.*, **47**, 1 (2008).
22. C. T. Kresge, M. E. Leonowicz, W. J. Roth, J. C. Vartuli and J. S. Beck, *Nature*, **359**, 710 (1992).
23. P. T. Tanev, M. Chibwe and T. J. Pinnavaia, *Nature*, **368**, 321 (1994).
24. P. Yang, D. Zhao, D. I. Margolese, B. F. Chmelka and G. D. Stucky, *Nature*, **396**, 152 (1998).
25. M. Kim, M. Bertram, M. Pollmann, A. V. Oertzen, A. S. Mikhailov, H. H. Rotermund and G. Ertl, *Science*, **292**, 1357 (2001).
26. E. E. Bloch, W. L. Queen, R. Krishna, J. M. Zarozny, C. M. Brown and J. R. Long, *Science*, **335**, 1606 (2012).
27. M. Mapa and C. S. Gopinath, *Chem. Mater.*, **21**, 351 (2008).
28. A. Ashcroft, A. Cheetham and M. Green, *Nature*, **352**, 225 (1991).
29. S. H. Joo, J. Y. Park, C.-K. Tsung, Y. Yamada, P. Yang and G. A. Somorjai, *Nature Mater.*, **8**, 126 (2008).
30. W. H. Suh and K. S. Suslick, *J. Am. Chem. Soc.*, **127**, 12007 (2005).
31. D. S. Jung, S. B. Park and Y. C. Kang, *Korean J. Chem. Eng.*, **27**, 1621 (2010).
32. J. Y. Yun, A. S. Reddy, S. Yang, H. J. Kim, H. Y. Koo, H. M. Lee, C. H. Jung, K. Qadir, S. Kim and J. Y. Park, *Catal. Lett.*, **142**, 326 (2012).
33. K. Okano, S. Koizumi, S. R. P. Silva and G. A. Amaratunga, *Nature*, **381**, 140 (1996).
34. A. M. Morales and C. M. Lieber, *Science*, **279**, 208 (1998).
35. R. Mueller, L. Mädler and S. E. Pratsinis, *Chem. Eng. Sci.*, **58**, 1969 (2003).
36. P. L. J. Gunter, J. W. Niemantsverdriet, F. H. Ribeiro and G. A. Somorjai, *Cat. Rev.-Sci. Eng.*, **39**(1-2), 77 (1997).
37. A. Y. Stakheev and L. M. Kustov, *Appl. Catal. A: Gen.*, **188**, 3 (1999).
38. P. Forzatti and L. Lietti, *Catal. Today*, **52**, 165 (1999).
39. J. N. Kuhn, C.-K. Tsung, W. Huang and G. A. Somorjai, *J. Catal.*, **265**, 209 (2009).
40. J. H. Bang, Y. T. Didenko, R. J. Helmich and K. S. Suslick, *Material Matters*, **7**, 15 (2012).